Proton Transfer Limits Protein Translocation Rate by the Thylakoid ΔpH/Tat Machinery

Siegfried M. Musser‡ and Steven M. Theg*

Division of Biological Sciences, Section of Plant Biology, University of California, One Shields Avenue Davis, California 95616

Received January 19, 2000; Revised Manuscript Received April 26, 2000

ABSTRACT: The thylakoid transmembrane ΔpH is the sole energy source driving translocation of precursor proteins by the ΔpH/Tat machinery. Consequently, proton translocation must be coupled to precursor translocation. For the precursor of the 17 kDa protein of the oxygen-evolving complex (pOE17), the protein translocation process is characterized by a steep drop in efficiency at an external pH below 7.0 and above 8.7. As the membrane ΔpH is virtually unaffected from pH 6.5 to 9.2, the loss in import efficiency is a consequence of the titration of multiple residues within the translocation machinery. Transport is retarded by a factor of 2−3 in deuterium oxide (D_2O) relative to water, strongly suggesting that proton-transfer reactions limit translocation rate. The solvent isotope effect manifests itself after the precursor binds to the membrane, indicating that the rate-limiting step is a later event in the transport process.

Two distinct translocation machineries transport precursor proteins across the thylakoid membrane from the stroma into the lumen, the cpSec machinery and the cpTat machinery (a.k.a. the ΔpH-dependent translocase). Homologous translocation machineries are utilized to export precursor proteins from the *Escherichia coli* cytoplasm to the periplasmic space and are denoted the Sec and Tat machineries, respectively. In bacteria, the Sec translocase consists of two trimeric integral membrane domains, SecYEG and SecDFyajC, and the peripheral ATPase SecA (*1*−*6*). Though the cpSec machinery has not received as much attention, SecA, SecY, and SecE protein homologues exist in higher plant plastids (*7*−*9*). ATP hydrolysis by SecA is essential for Sec transport, yet a proton motive force (pmf)[1] improves transport rate and energetic efficiency (*2, 10*−*14*). SecA is responsible for initiation of translocation, a task accomplished through major conformational changes resulting in the insertion of two large SecA domains (30 and 65 kDa) into the translocase with the bound leader sequence (*15, 16*). ATP hydrolysis is required for release of the preprotein from membrane-associated SecA; the pmf reduces the SecA/SecYEG affinity, thereby promoting SecA release from the translocase (*17, 18*). The pmf also drives later steps of translocation in the absence of SecA and ATP hydrolysis. The exact roles of the $\Delta\psi$ and ΔpH components of the pmf in these later steps of precursor translocation have not been deciphered as they are precursor protein dependent, although $\Delta\psi$-driven electrophoretic movement appears to be utilized in some cases (*11, 13, 19*−*24*). Note that it is unlikely that a $\Delta\psi$ plays a role in cpSec transport due to the low steady-state $\Delta\psi$ maintained across the thylakoid membrane in the light (*25*). While the decrease in ΔpH observed during translocation initiation in bacteria (*26*) could be explained by simple leakage resulting from the presence of a large protein molecule within the translocation pore, no model has yet been proposed to explain the decreased translocation rate observed in D_2O (*27*), a result that supports a direct role for rate-limiting proton transfer in ΔpH-driven translocation. A tightly coupled protein/proton antiporter activity is an enticing possibility, although it is difficult to reconcile with the observed protein dependence of pmf stimulated transport (*11*, *21*−*23*).

In contrast to the (cp)Sec machinery, translocation by the cpTat machinery requires energetic input only from the presence of a ΔpH across the membrane—nucleotide triphosphate hydrolysis is not utilized in any way by this machinery. The membrane ΔpH is the dominant contributor to the pmf in thylakoids (*25*), and in fact, collapse of the small, exisiting $\Delta\psi$ across the thylakoid membrane has no measurable effect on Tat transport efficiency (*28*). From an energetic standpoint alone, then, it can be concluded that the energetic cost of Tat precursor transport is derived from the exit of protons from the lumen/periplasm in exchange for precursor transport. This antiport exchange of protons for precursor must be well-controlled, for a dramatic increase in ionic permeability during precursor transport would ruin the energy-transducing power of the membranes in which these transport machineries reside. In fact, the conductance of an individual cpTat translocase during precursor transport has been observed to be less than a few picosiemens (*29*).

† This work was supported by National Research Service Award 1-F32-GM18135 from the National Institute of General Medical Sciences (S.M.M.) and by U.S. Department of Agriculture Grant 95-37304-2325 (S.M.T.).

* To whom correspondence should be addressed: phone (530) 752-0624; fax (530) 752-5410; e-mail smtheg@ucdavis.edu.

‡ Present address: Department of Biochemistry, MS 009, Brandeis University, Waltham, MA 02454.

[1] Abbreviations: pmf, proton motive force; pOE17, precursor for the 17 kDa protein of the oxygen-evolving complex; pL (L = lyonium), equivalent pH for solutions with protium and deuterium isotopes; ΔpH, transmembrane pH gradient; $\Delta\psi$, transmembrane electrical potential.

10.1021/bi000115f CCC: $19.00
Published on Web 06/21/2000

Though the oligomeric structure of the Tat machinery is still unknown, the *E. coli* proteins TatA/E (Tha4), TatB (Hcf106), and TatC (maize homologues in parentheses) have been demonstrated to be involved in Tat precursor transport through genetic approaches (*30*−*35*). It is still unknown whether another protein encoded by the bacterial *Tat* operon, TatD (*32*), has any role in the Tat precursor translocation process. TatD appears to be a soluble protein (*32*). The TatA/E (Tha4) and TatB (Hcf106) proteins are membrane-bound with the bulk of the C-terminal portion on the cytoplasmic (stromal) side of the membrane, in agreement with hydropathy profiles (*30, 35*). TatC with its six putative transmembrane spans (*32*) is the most likely known protein to form the core of the membrane-bound translocation complex.

Described here are experiments designed to investigate the role of protons in the cpTat-catalyzed protein translocation process. The import efficiency of the pOE17 precursor shows a strong dependence on external pH that is not a consequence of reaching a threshold ΔpH for transport. Consequently, the pK_a values obtained from the pH dependence of import efficiency reflect the protonation state of residues within the transport machinery required for transport. A 2−3-fold decrease in import rate in D_2O relative to H_2O strongly suggests that proton transfers are involved in crucial, rate-limiting steps of the protein transport process.

MATERIALS AND METHODS

Materials. The precursor protein pOE17(C)-BioHis was overexpressed in *E. coli* strain BL21(DE3) [F^- *ompT hsdSB* (r_B^- m_B^-) *gal dcm* (DE3)] in the presence of 0.5 mCi/mL [^{3}H]leucine (NEN-DuPont) and stored in 8 M urea, and 200 mM sodium phosphate, pH 7.0, as described (*36*). This precursor protein contains a C-terminal His_6 tag on the full-length maize precursor of the 17 kDa protein of the oxygen evolving complex (pOE17).

Thylakoid Import Assays. Chloroplasts and thylakoids were isolated from pea seedlings (*36*). For D_2O experiments, thylakoids were resuspended with the desired D_2O buffer and washed at least once. Thylakoid suspensions were kept at about 6 °C instead of on ice to avoid freezing D_2O solutions (pure D_2O freezing point is 3.8 °C). Unless otherwise indicated, precursor translocation into thylakoids was assayed in import buffer (IB; 50 mM Tricine, 330 mM sorbitol, and 3 mM $MgCl_2$) by inaccessibility of the mature protein to externally added thermolysin and analyzed by SDS−PAGE and fluorography as described (*36*).

Data Analysis. Data were fitted with the least-squares algorithm of KaleidaGraph. The pL vs imported protein (I) data of Figure 1C were fitted with $I = I_{max}/(1 + 10^{n_1(pK_{a1}-pL)} + 10^{n_2(pL-pK_{a2})})$, which assumes *n* equivalent protons involved in simultaneous protonation/deprotonation according to the Henderson−Hasselbalch formulation (*37*).

Δ*pH Measurements.* Thylakoid membrane ΔpH was calculated from the fluorescence of 9-aminoacridine (*25*) on an SLM AMINCO−Bowman series 2 luminescence spectrometer (λ_{ex} = 420 nm; λ_{em} = 528 nm) at the onset of actinic illumination (> 635 nm) provided with a Schott KL1500 halogen lamp. Thylakoid lumenal volume was estimated as 20 μL/mg of chlorophyll (*25, 38, 39*).

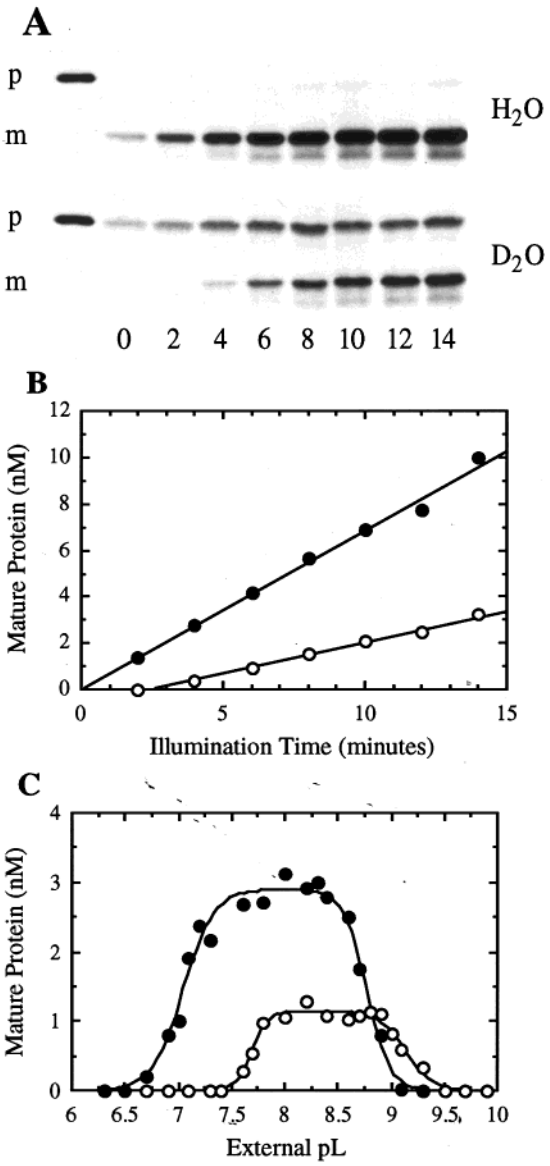

FIGURE 1: pL dependence of pOE17(C)-BioHis thylakoid import. (A) ^{3}H-pOE17(C)-BioHis (100 nM) was preincubated with thylakoids (0.3 mg/mL chlorophyll) in IB (pH 8.0/pD 8.4) for 8 min in the dark. Thylakoid import was initiated by illumination and aliquots were quenched with a 10-fold excess of IB containing thermolysin at the indicated time points. The leftmost lane corresponds to 2.5% of the precursor added to the reaction. (B) Quantitation of the data shown in panel A. (C) Ten microliters of thylakoid suspension (1.8 mg/mL chlorophyll) in weakly buffered medium (5 mM Tricine, 330 mM sorbitol, and 3 mM $MgCl_2$, pH 7.8/pD 8.2) was mixed with 3 μL of 2 μM ^{3}H-pOE17(C)-BioHis in the same medium and 47 μL 50 mM Tricine, 50 mM Bis-tris propane, 330 mM sorbitol, and 3 mM $MgCl_2$ of the indicated pL and incubated in the dark for 8 min. Samples were then illuminated for 12 min. Data were fitted as described under Materials and Methods. (●) H_2O, (○) D_2O. Note that the incomplete digestion of full-length precursor for the D_2O samples in panel A is indicative of the reduced protease activity in the deuterated buffer. This lower activity does not affect the validity of the quantitation (B) since the mature protein is not susceptible to digestion.

Other. Deuterium oxide solutions were prepared by solubilizing reagents in D_2O (99.9%, Aldrich) and, by use of a hydrogen-ion-selective glass electrode, adjusted to the desired pD with NaOD or DCl (pD = pH meter reading + 0.4) (*40*).

RESULTS AND DISCUSSION

Deuterium Solvent Isotope Effect. It was shown earlier that a thylakoid import time course for pOE17(C)-BioHis is linear immediately after reaction initiation if the precursor protein is preincubated with thylakoids in the dark (*36*), and thus all import experiments described here included such a preincubation. In both H_2O and D_2O buffers, maturation of pOE17(C)-BioHis in the presence of thylakoids was linear for over 10 min, though the translocation rate in D_2O was found to be consistently lower by a factor of 2−3 (Figure 1A,B). This lower translocation rate does not arise from the higher macroscopic viscosity of D_2O, as determined by increasing the viscosity of H_2O buffers with sorbitol (data not shown). The approximate 2-min lag in onset of import activity in D_2O was consistently observed (three independent experiments) and therefore is considered a feature of the isotope effect. When enzymatic activity is compared in deuterium and protium buffers, the kinetics should ideally be measured at the peaks of the respective pL (where L = D or H) rate profile to ensure that the enzyme ionization state is identical for the two situations (*37*). The pH and pD rate profiles for pOE17(C)-BioHis thylakoid import have the same general shape (Figure 1C). A small window of maximum import velocity with a width of only about 1 pL unit was observed. The import time courses of Figure 1A were performed at a pL that approximates the peak for the two pL profiles, i.e., pH = 8.0 and pD = 8.4.

Membrane ΔpL vs External pH and D_2O Concentration. As the energetic requirement for translocation of pOE17 into the thylakoid lumen is provided by the membrane ΔpH, the membrane ΔpH as a function of the external pH was examined with 9-aminoacridine (*25*). The fact that there was virtually no change in the membrane ΔpH generated when the external pH was varied from 6.25 to 9.25 (Figure 2A) indicates that the drop in import efficiency below pH 7.0 and above pH 8.7 (Figure 1C) is indeed a consequence of changes in ionization state of residues within the translocation machinery (or, less likely, within the precursor protein) rather than a consequence of energetic considerations. The decreased ΔpH observed by this method at pH 9.5 has been observed earlier (*38*) and is most likely a consequence of invalidity of the technique near the pK_a (=9.9) of 9-aminoacridine (*25*). In addition, examination of the isotopic dependence of the ΔpL indicated that generation of ΔpL by the photosynthetic reactions is identical in protium and deuterium buffers (Figure 2B). The onset and relaxation of the ΔpL is likewise identical (data not shown), indicating that the delay in precursor translocation in D_2O buffer upon illumination (Figure 1B) is a consequence of some intrinsic property of the translocation machinery rather than a slower buildup of the energetic driving force. The implication is that the lower steady-state import efficiency observed in D_2O relative to H_2O buffers is a consequence of an isotopic effect on the enzymatic functioning of the translocation machinery rather than the availablity of energy for transport.

One might justifiably question the relevence of the ΔpL measurements (Figure 2) on the thylakoid import experiments (Figure 1) since the experimental designs were different and import and ΔpL were not measured simultaneously. Differences in light intensity (lower intensity for import reactions) and photon energy (white vs red light for import and ΔpL

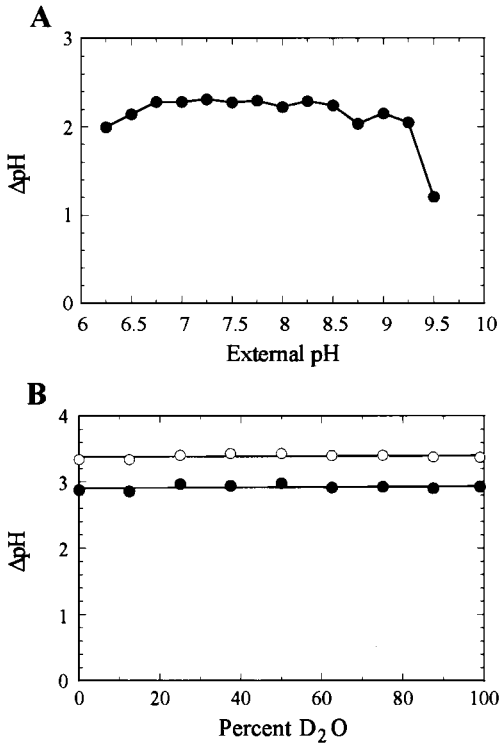

FIGURE 2: ΔpL dependence on external pH and D_2O concentration. (A) The 9-aminoacridine method was utilized to measure thylakoidal transmembrane ΔpH as a function of external pH in a solution containing 20 μM 9-aminoacridine, 20 μg/mL chlorophyll, 50 mM Tricine, 50 mM Bis-tris propane, 330 mM sorbitol, and 3 mM $MgCl_2$. (B) (●) Transmembrane ΔpL was measured as a function of the D_2O composition by mixing appropriate volumes of H_2O and D_2O buffers containing 20 μM 9-aminoacridine, 50 mM Tricine, 330 mM sorbitol, and 3 mM $MgCl_2$, at pH 8.0 or pD 8.4, respectively. (○) Same experiment including 40 μM methyl viologen.

measurements, respectively) could potentially make the results incomparable. For example, if the sustained ΔpH in H_2O under the import conditions is near a threshold ΔpH for transport below which import efficiency drops dramatically, a small decrease in ΔpL upon changing the solvent to D_2O could result in a dramatic decrease in import efficiency. Earlier work with lettuce thylakoids, however, has demonstrated that the measured ΔpL is virtually identical over a wide range of light intensities in the presence of methyl viologen (*41*), an electron acceptor that results in net oxygen uptake (*42*). Our data also shows that ΔpL is invariant in H_2O and D_2O buffers in the presence of methyl viologen (Figure 2B). As an additional test, import efficiency was measured in the presence of methyl viologen (Figure 3). Under these import conditions, the ΔpL is undoubtedly greater (the nonzero y-intercept reflects the greater sensitivity to light leaks during preincubation sample manipulation due to the presence of methyl viologen), and yet the import efficiency is still decreased ~2-fold in D_2O relative to H_2O. These data indicate that the decreased import efficiency in D_2O is a real effect of the heavier isotope on enzymatic activity. Note that the absolute value of the measured ΔpL varied from about 2 to 3 depending on thylakoid preparation but was consistently above 3 when methyl viologen was included as an electron acceptor. This variability in ΔpL

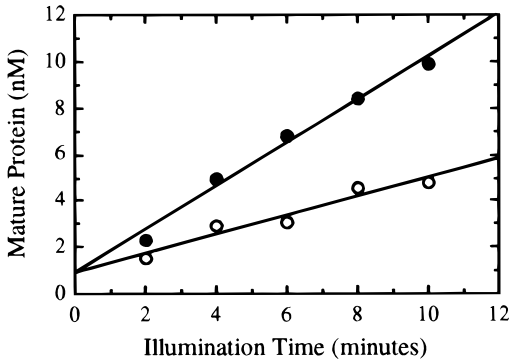

FIGURE 3: Import time course with ethyl viologen. Results from the same experiment as in Figure 1A except with 40 μM methyl viologen. (●) H_2O; (○) D_2O.

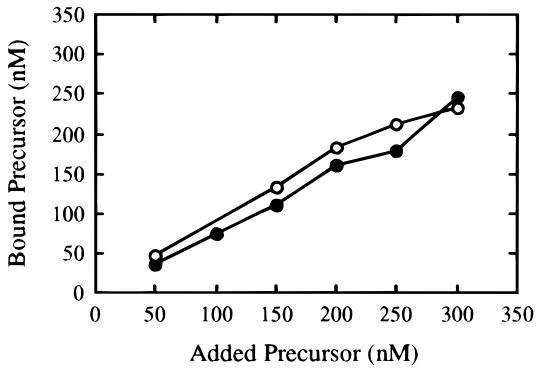

FIGURE 4: Precursor bound to the thylakoid membrane. The indicated ^{3}H-pOE17(C)-BioHis concentration was incubated with thylakoids (0.3 mg/mL chlorophyll) in IB for 12 min in the dark at room temperature. Samples were diluted with an equal volume of ice-cold IB with 2 μM carbonyl cyanide *m*-chlorophenylhydrozone (CCCP) and immediately microcentrifuged for 20 s. Pellets were analyzed by SDS−PAGE and fluorography. (●) H_2O; (○) D_2O.

could explain some of the observed variability in the solvent isotope effect on import efficiency.

The Isotope Effect Manifests Itself after the Membrane Binding Event. The initial interaction of precursor with the thylakoid membrane occurs in the absence of light, and consequently, with no membrane ΔpH (*36*). The possibility that the initial binding interaction is perturbed in D_2O solvent and thereby leads to the observed isotope effect could therefore be directly addressed. It was found that the amount of precursor that bound to the thylakoid membrane in the dark was essentially the same in H_2O or D_2O buffer (Figure 4). While the import velocity saturates at about 100 nM in both H_2O and D_2O and the observed K_m is essentially equivalent in the two situations (data not shown), the amount of precursor bound to the membrane continues to increase linearly with increasing precursor concentration well beyond 100 nM (Figure 4). The implication of these data is that the number of binding sites for precursor on the membrane substantially exceeds the number of translocons. Earlier work demonstrated that the majority, if not all, of this membrane-bound precursor is import-competent (*36*). The kinetic step slowed in deuterated solvent must therefore occur after the initial binding interactions.

pL Rate Profile Transitions. The experiment described in Figure 1C reveals that there is a strong pH dependence to precursor transport efficiency, with transport efficiency dropping rapidly below pH 7.0 and above pH 8.7. As the membrane ΔpH is unaffected at these transition points (Figure 2), the sharp transitions in these data indicate that the ionization state of multiple residues plays a vital role in the precursor translocation process. By use of the Henderson−Hasselbalch equation and assuming that the chemical groups responsible for the transition are simultaneously dissociated (i.e., cooperatively) with identical pK_a values, it was found that the number of protons involved in all cases averages around 3−4 (n_1 and n_2 of Table 1); we observed that the accuracy of the fitting procedure dropped dramatically for n larger than 2. These data can be explained by (1) titration of n chemically distinct residues with similar pK_a values or (2) titration of n chemically identical residues. While it is possible that these titrating residues merely indicate that the enzyme complex must be in a specific ionization state for protein transport to occur, it is also possible that these residues are alternately protonated and deprotonated during the turnover cycle. As an example of the second possibility, a situation in which one residue in each unit of a homotrimeric complex undergoes protonation/deprotonation during turnover (i.e., $n_1 = n_2 = 3$) would be consistent with the data. Even more enticing is the possibility that the protonation/deprotonation events are directly coupled to the protein transport process. Multiple protonations/deprotonations of each residue could occur during a single protein translocation event such that the proton/protein ratio is greater than 3−4.

Table 1: Parameters Characterizing the pL Dependence of Thylakoid Import Efficiency[a]

	pK_{a1}	n_1	pK_{a2}	n_2
H_2O	7.04 (0.01)	3.58 (0.80)	8.69 (0.11)	3.42 (0.77)
D_2O	7.70 (0.01)	4.28 (2.26)	8.99 (0.21)	2.48 (1.45)
ΔpK_a	0.66		0.30	

[a] Values determined as described in Figure 1 are given as an average of two independent determinations with standard deviations in parentheses. One set of measurements consists of the data in Figure 1, whereas the other utilized 50 mM Mops, 50 mM Mes, 50 mM Taps, and 5 mM $MgCl_2$ as the import buffer.

The pK_a values estimated from the fits to the pL profile data (Figure 1C) provide an indication of residues likely to be titrating at the transition points. Histidine (p$K_a \approx 6.0$−7.0) and cysteine (p$K_a \approx 9.0$−9.5) or tyrosine (p$K_a \approx 10.0$−10.3) (*43*) are reasonable candidates for residues titrating at the lower and higher pH values, respectively. In D_2O, the limiting pD values are 7.7 and 9.0, respectively, corresponding to pK_a shifts of 0.66 and 0.30 (Table 1). For such isotopic solvents, histidine and tyrosine would be expected to have pK_a shifts from 0.4 to 0.6, although values outside this range are possible as a consequence of environmental perturbations (*37*, *40*). Cysteine has a notably lower ΔpK_a of ∼0.3 due to sulfhydryls' lower affinity for deuterium than protium (*37*, *44*). Thus, the pK_a and ΔpK_a values together are most readily reconciled with histidine and cysteine residue protonation/deprotonation at the two observed transitions in the pL profiles. As there are no conserved histidines or cysteines (or even tyrosines) in any of the Tat machinery proteins (TatABCD), there exists the possibility that additional component(s) of the Tat machinery remain to be identified. Alternatively, it is noteworthy that the TatC residues E15 and R19 (*E. coli* nomenclature) are conserved and R17 and D211 are functionally conserved (R/K and D/E, respectively). Significant perturbations to solution pK_a values for these

residues could result from the protein's three-dimensional structure. One of these residues, therefore, could be titrating at the transition points in the pL rate profiles.

Interpretation of the Solvent Isotope Effect. Musser and Theg (*36*) postulated a model of the translocation process wherein the precursor diffuses to the transport machinery after first binding elsewhere on the membrane surface. This model can be summarized as follows:

$$P + TM \xrightarrow{1} (P{\cdot}TM)_S \xrightarrow{2} (P{\cdot}TM)_T \xrightarrow{3} M + TM$$

where P is the full-length precursor, TM is the thylakoid membrane, $(P{\cdot}TM)_S$ and $(P{\cdot}TM)_T$ denote the precursor bound to the TM surface and the transport machinery, respectively, and M represents the mature protein. Though there are three steps in this reaction sequence, only two kinetic steps have been distinguished experimentally (*36*); the first kinetic phase occurs in the absence of the pmf (e.g., 1 alone, or 1 and 2) and the second phase requires the pmf (e.g., 2 and 3, or 3 alone). Solvent isotope effects can arise from perturbations to reactant-state or transition-state populations (*37*). For a complex sequence of reactions such as protein translocation, it is difficult to dissect the isotope effect because results from perturbations to either population can yield the same result. The initial binding interaction of pOE17 with the thylakoid membrane (first kinetic phase) was shown here to be unaffected in D_2O (Figure 4), demonstrating that there are no isotopic reactant-state perturbations up to this point in the translocation pathway. While it is not possible to rule out isotopic reactant-state perturbations after the membrane binding reaction from the reported data, such effects are usually small (e.g., <1.5) (*37*). Isotope effects of 2−4 are common, however, for enzyme reactions that involve proton transfer (*37*). Thus, rate-limiting proton transfer is considered a likely explanation for the isotope effects observed here. It is possible, in fact, that proton transfers mediated by the residues responsible for the pH dependence of precursor translocation efficiency could give rise to the observed isotope effect.

Proton transfers in solution typically occur at a diffusion-controlled rate ($\sim 10^{10}$ M^{-1} s^{-1}), so it is intriguing that the translocation process, occurring on the time scale of seconds, could be rate-limited by the proton transfer rate. It is unlikely that the kinetics of membrane binding (reaction 1) show a solvent kinetic isotope effect because earlier data demonstrated that this interaction is hydrophobic in nature, thereby suggesting that proton transfers are not involved (*36*). From a theoretical standpoint alone, the diffusional reactions 1 and 2 are unlikely to be controlled by proton transfer; a mechanism would have to exist whereby inherently rapid proton transfers would be dramatically slowed. However, the proton motive force could be directly coupled to protein transport in a situation where protons are passed down a concentration gradient in exchange for protein translocation (reaction 3). This passage of protons across the membrane, carefully controlled by a proteinaceous machinery, could quite reasonably be susceptible to a deuterium solvent kinetic isotope effect. Further experiments are clearly required to work out the molecular details of this complex enzymatic reaction.

NOTE ADDED IN PROOF

After this paper had been accepted for publication a study appeared in which it was shown that TatD is not involved in protein transport in *E. coli* (*45*).

REFERENCES

1. Ito, K. (1996) *Genes Cells 1*, 337−346.
2. Wickner, W., and Leonard, M. R. (1996) *J. Biol. Chem. 271*, 29514−29516.
3. Duong, F., Eichler, J., Price, A., Leonard, M. R., and Wickner, W. (1997) *Cell 91*, 567−573.
4. Danese, P. N., and Silhavy, T. J. (1998) *Annu. Rev. Genet. 32*, 59−94.
5. Driessen, A. J. M., Fekkes, P., and van der Wolk, J. P. W. (1998) *Curr. Opin. Microbiol. 1*, 216−222.
6. Economou, A. (1998) *Mol. Microbiol. 27*, 511−518.
7. Laidler, V., Chaddock, A. M., Knott, T. G., Walker, D., and Robinson, C. (1995) *J. Biol. Chem. 270*, 17664−17667.
8. Voelker, R., Mendel-Hartvig, J., and Barken, A. (1997) *Genetics 145*, 467−478.
9. Schuenemann, D., Amin, P., Hartmann, E., and Hoffman, N. E. (1999) *J. Biol. Chem. 274*, 12177−12182.
10. Duong, F., and Wickner, W. (1997) *EMBO J. 16*, 2756−2768.
11. Ernst, F., Hoffschulte, H. K., Thome-Kromer, B., Swidersky, U. E., Werner, P. K., and Müller, M. (1994) *J. Biol. Chem. 269*, 12840−12854.
12. Akimaru, J., Matsuyama, S., Tokuda, H., and Mizushima, S. (1991) *Proc. Natl. Acad. Sci. U.S.A. 88*, 6545−6549.
13. Schiebel, E., Driessen, A. J. M., Hartl, F.-U., and Wickner, W. (1991) *Cell 64*, 927−939.
14. Bassilana, M., and Wickner, W. (1993) *Biochemistry 32*, 2626−2630.
15. Eichler, J., and Wickner, W. (1997) *Proc. Natl. Acad. Sci. U.S.A. 94*, 5574−5581.
16. Economou, A., and Wickner, W. (1994) *Cell 78*, 835−843.
17. Nishiyame, K., Fukuda, A., Morita, K., and Tokuda, H. (1999) *EMBO J. 18*, 1049−1058.
18. Duong, F., and Wickner, W. (1999) *EMBO J. 18*, 3263−3270.
19. Andersson, H., and von Heijne, G. (1994) *EMBO J. 13*, 2267−2272.
20. Cao, G., Kuhn, A., and Dalbey, R. E. (1995) *EMBO J. 14*, 866−875.
21. Daniels, C. J., Bole, D. G., Quay, S. C., and Oxender, D. L. (1981) *Proc. Natl. Acad. Sci. U.S.A. 78*, 5396−5400.
22. Yamada, H., Tokuda, H., and Mizushima, S. (1989) *J. Biol. Chem. 264*, 1723−1728.
23. Yamade, K., Ichihara, S., and Mizushima, S. (1987) *J. Biol. Chem. 262*, 3107−3111.
24. Schuenemann, T. A., Delgado-Nixon, V. M., and Dalbey, R. E. (1999) *J. Biol. Chem. 274*, 6855−6864.
25. Mills, J. D. (1986) in *Photosynthesis, Energy Transduction: A Practical Approach* (Hipkins, M. F., and Baker, N. R., Eds.) pp 143−187, IRL Press, Washington, DC.
26. Kawasaki, S., Mizushima, S., and Tokuda, H. (1993) *J. Biol. Chem. 268*, 8193−8198.
27. Driessen, A. J. M., and Wickner, W. (1991) *Proc. Natl. Acad. Sci. U.S.A. 88*, 2471−2475.
28. Cline, K., Ettinger, W. F., and Theg, S. M. (1992) *J. Biol. Chem. 267*, 2688−2696.
29. Teter, S. A., and Theg, S. M. (1998) *Proc. Natl. Acad. Sci. U.S.A. 95*, 1590−1594.
30. Settles, A. M., Yonetani, A., Baron, A., Bush, D. R., Cline, K., and Martienssen, R. (1997) *Science 278*, 1467−70.
31. Mori, H., Summer, E. J., Ma, X., and Cline, K. (1999) *J. Cell Biol. 146*, 45−55.
32. Sargent, F., Bogsch, E. G., Stanley, N. R., Wexler, M., Robinson, C., Berks, B. C., and Palmer, T. (1998) *EMBO J. 17*, 3640−3650.
33. Weiner, J. H., Bilous, P. T., Shaw, G. M., Lubitz, S. P., Frost, L., Thomas, G. H., Cole, J. A., and Turner, R. J. (1998) *Cell 93*, 93−101.

34. Bogsch, E. G., Sargent, F., Stanley, N. R., Berks, B. C., Robinson, C., and Palmer, T. (1998) *J. Biol. Chem. 273*, 18003−18006.
35. Walker, M. B., Roy, L. M., Coleman, E., Voelker, R., and Barkan, A. (1999) *J. Cell Biol. 147*, 267−275.
36. Musser, S. M., and Theg, S. M. (1999) *Eur. J. Biochem.* (in press).
37. Quinn, D. M., and Sutton, L. D. (1991) in *Enzyme Mechanism for Isotope Effects* (Cook, P. F., Ed.) pp 73−126, CRC Press, Boca Raton, FL.
38. Schuldiner, S., Rottenberg, H., and Avron, M. (1972) *Eur. J. Biochem. 25*, 64−70.
39. Portis, A. R., and McCarty, R. E. (1974) *J. Biol. Chem. 249*, 6250−6254.
40. Schowen, K. B., and Schowen, R. L. (1982) *Methods Enzymol. 87*, 551−606.
41. Haraux, F., and de Kouchkovsky, Y. (1982) *Biochim. Biophys. Acta 679*, 235−247.
42. Allen, J. F., and Holmes, N. G. (1986) in *Photosynthesis, Energy Transduction: A Practical Approach* (Hipkins, M. F., and Baker, N. R., Eds.) pp 103−141, IRL Press, Washington, DC.
43. Creighton, T. E. (1993) *Proteins: Structures and Molecular Properties*, W. H. Freeman and Co., New York.
44. Venkatasubban, K. S., and Schowen, R. L. (1983) *CRC Crit. Rev. Biochem. 17*, 1−44.
45. Wexler, M., Sargent, F., Jack, R. L., Stanley, N. R., Bogsch, E. G., Robinson, C., Berks, B. C., and Palmer, T. (2000) *J. Biol. Chem. 275*, 16717−16722.

BI000115F